

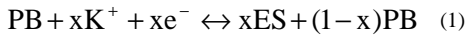
## Interpretation of Variable Diffusivity Observed at the Prussian Blue Electrode during the Insertion/Extraction Processes

Lin-Chi Chen and Kuo-Chuan Ho\*

Department of Chemical Engineering  
National Taiwan University  
Taipei 10617, Taiwan

### Introduction

Prussian blue (PB,  $K_4Fe(CN)_6$ ), being investigated for electrochromic, battery, and ionic sensing applications, is an ideal compound for studying the redox insertion processes, because PB can reversibly be reduced to colorless Everitt's salt (ES,  $K_2Fe(CN)_6$ ) with the simultaneous insertion of  $K^+$  into the PB lattice. Accordingly, the PB/ES change can be described as follows:



where  $x$  represents the insertion level of  $K^+$  or the conversion of ES and can be determined from the absorptometric study (at 690 nm).

Recently, we observed that the apparent diffusivity ( $D$ ), measured at the PB/SnO<sub>2</sub> glass electrode in 1N KCl + 0.01N HCl, varied with the potential applied ( $E$ ) [1]. (See Fig. 1(a), this measurement was performed using the potentiostatic intermittent titration technique (PITT) - chronoabsorptometry. It was also found that the minimum diffusivity occurred near the voltammetric peak potential. Moreover, the peak-shaped D-E relationship was also noticed among Li<sup>+</sup>-inserted electrodes [2]. This infers that such a D-E relationship is likely to be a common phenomena for other insertion compounds. Therefore, our chief aim is to develop a model in explaining the variable diffusivity at the PB electrode and to help in predicting the peak-shaped D-E relationship during the insertion/extraction processes.

### Model

McCargar *et al.* [3] proposed that a partially reduced PB film could be considered as a binary, solid solution of PB and ES. It was also shown that the binary solution model gave good E-x fits. This inspires us to explain the variable diffusivity, shown in Fig. 1(a), based on the binary diffusion theory. According to this theory, the following relationship can be obtained [4]

$$D_{12} = D_{12}^0 \left[ 1 + \frac{x(1-x)}{RT} \left( \frac{\partial^2 \underline{G}^{ex}}{\partial x^2} \right) \right] \quad (2)$$

where  $D_{12}$  and  $D_{12}^0$  represent the apparent and intrinsic binary diffusivity, respectively. Eq.(2) suggests that the measured diffusivity,  $D_{12}$ , is an implicit function of the potential due to the composition dependency of the potential. Furthermore,  $D_{12}$  is also affected by the excess property of PB-ES mixing,  $\underline{G}^{ex}$ , which also depends on the composition, and thus the potential.

### Results and Discussions

To examine the applicability of Eq.(2), various kinds of free energy given in Fig. 2 were calculated from the following equation:

$$\Delta \underline{G}^m = -F \int_0^x [E(x) - E_0] dx = \Delta \underline{G}^{idm} + \underline{G}^{ex} \quad (3)$$

where  $E(x)$  was determined experimentally and is given in Fig. 1(b);  $E_0$  is the standard potential of Eq.(1). By substituting the excess property into Eq.(2) along with Fig. 1(a), a satisfied D-x fit was obtained as shown in Fig. 3. The predicted curve fits well with the experimental result in the range  $0.1 < x < 0.9$ . It also predicts the concavity of the D-x curve.

Actually, Eq.(2) reveals that the D-x (or D-E) and  $\underline{G}^{ex}$ -x (or  $\underline{G}^{ex}$ -E) curves possess the opposite concavity. That is, a concave-down D-x behavior is attributed to the concave-up  $\underline{G}^{ex}$ -x relationship. This totally agrees with our data shown in Fig. 2 and Fig. 3. It is noticed from Fig.2 that the global  $\underline{G}^{ex}$ -x curve is characterized by a concave-up trend, but the  $\underline{G}^{ex}$ -x behavior in the vicinity of  $x = 0.5$  is concave downward. This means that the change in global excess property tends to increase the entropy and to enhance the diffusion process; however, the local concave-down  $\underline{G}^{ex}$ -x behavior suppresses the PB-ES mixing and results in a concave-up D-x relationship.

Through the above analysis, it is known that not only the E-x relationship [3] but also the D-x behavior of the PB/ES redox process can be explained by the binary solution thermodynamics. Nonetheless, it is worthwhile to mention that the excess property as shown in Fig. 2 is asymmetric, whereas the strictly regular solution model with a symmetric

$\underline{G}^{ex}$ -x assumption was adopted in the literature [3]. Although the symmetric model is easier to explain the E-x relationship, it fails to predict the D-x curve. To overcome this drawback, a general expression, such as Eq.(2), is proposed as a realistic model for the apparent binary diffusivity.

### Conclusions

In addition to present a general, well-fitted model for the apparent binary diffusivity, implications concerning the diffusion mechanism are equally important. Of course, the pivotal conclusion about this work is the revelation that a D-x curve for an insertion reaction can easily be predicted from a diffusivity value at a given conversion and a given voltammogram (to provide the information of  $\underline{G}^{ex}$ -x), as long as the insertion electrode is analogous to PB.

### Acknowledgment

This work is being supported by the National Research Council of the Republic of China under Grant NSC 89-2214-E002-072.

### Key References

- [1] L.-C. Chen and K.-C. Ho, to be published in *J. Electrochem. Soc.* (2001).
- [2] D. Aurbach, M. D. Levi, E. Levi, H. Teller, B. Markovsky, G. Salitra, U. Heider, and L. Heider, *J. Electrochem. Soc.*, **145**, 3024 (1995).
- [3] J. W. McCargar and V. D. Neff, *J. Phys. Chem.*, **92**, 3598 (1988).
- [4] R. B. Bird, W. E. Stewart, and E. D. Lightfoot, *Transport Phenomena*, Wiley, USA (1960): Ch.18.

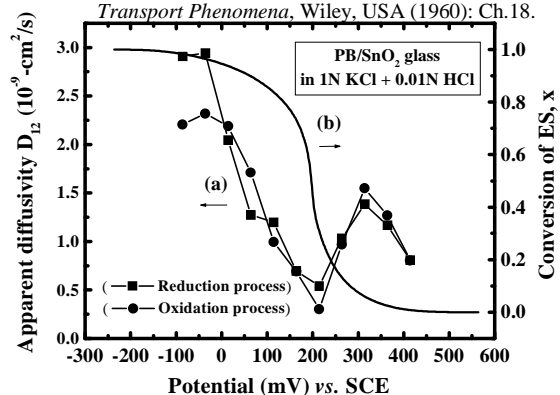


Fig. 1. (a) The equilibrated D-E curves measured using the PITT-chronoabsorptometry; (b) the pseudo-equilibrated x-E curve measured using the slow-scanned ( $\nu = 0.5$  mV/s) cyclic voltabsorptometry [1].

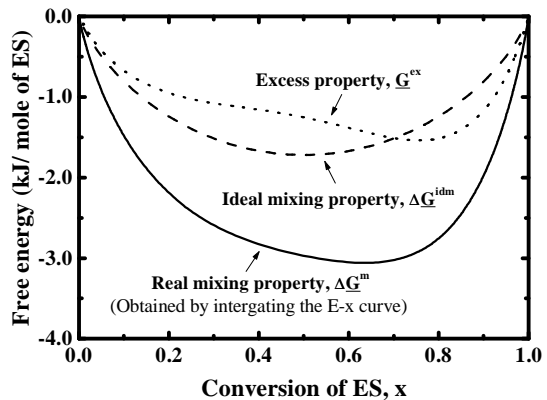


Fig. 2. The real-mixing, ideal-mixing, and excess thermodynamic properties, calculated according to Eq. (3) and Fig. 1(b). ( $E_0$  was determined to be 184.5 mV, whereas the voltammetric peak potential was observed to be ca. 198 mV vs. SCE.)

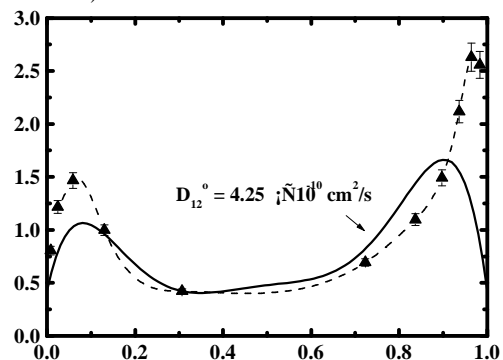


Fig. 3. A comparison between the experimental values of  $D_{12}$  and the model prediction from Eq.(2). The data points are the averaged values of the cathodic and anodic diffusivities taken from Fig. 1(a).